

Electronic Supplementary Information for

**PdMn bimetallic for low-energy electrocatalytic hydrogen generation coupled
with formate oxidation**

Hongjing Wang, Hongyong Chen, Qiqi Mao, Kai Deng, Hongjie Yu*, Xin Wang, You Xu,

Ziqiang Wang* and Liang Wang*

State Key Laboratory Breeding Base of Green-Chemical Synthesis Technology, College of
Chemical Engineering, Zhejiang University of Technology, Hangzhou 310014, P. R. China.

Corresponding authors

*E-mails: hongjieyu@zjut.edu.cn; zqwang@zjut.edu.cn; wangliang@zjut.edu.cn

Experimental section

Materials and chemicals: Manganese acetylacetonate ($\text{Mn}(\text{acac})_2$) was purchased from Alfa Aesar and Nafion solution (0.5 wt%) was obtained from Sigma-Aldrich. Sodium chloropalladate (Na_2PdCl_4), Manganese chloride (MnCl_2), ethylene glycol (EG), potassium hydroxide (KOH), diethylenetriamine (DETA) and N,N-dimethylformamide (DMF) were provided by Aladdin.

Synthesis of PdMn bimetalene: Typically, KOH (1 g) was first dissolved in EG (4 mL) and of DMF (5.9 mL) under ultrasonication, followed by adding Na_2PdCl_4 (300 μL , 0.1 M), $\text{Mn}(\text{acac})_2$ (5 mg) and DETA (5 mL) to the above solution. Then the mixed solution was injected into a Teflon lined reactor, which was heated to 200 °C and maintained for 8 h. Finally, the product was washed with ethanol/water for three cycles to remove redundant intermediates. For comparison, the Pd metallene was also prepared from the absence of Mn precursors, the PdMn bimetalene-L was also prepared from the presence of 2.5 mg $\text{Mn}(\text{acac})_2$ and the PdMn bimetalene-H was also prepared from the presence of 7.5 mg $\text{Mn}(\text{acac})_2$ in the similar synthesis conditions.

Characterizations: The morphology of catalysts was characterized via scanning electron microscope (SEM, Zeiss Gemini 500) and transmission electron microscope (TEM, JEM-2100 microscope). X-ray diffraction (XRD) was tested on the D8ADVANCE diffractometer. X-ray photoelectron spectroscopy (XPS) was performed by ESCALAB MK II spectrometer. Atomic force microscopy (AFM) was performed in tapping mode with a Multimode Nanoscope IIIa SPA. Inductively coupled plasma optical emission spectrometer (ICP-OES) was performed on a Hitachi model Agilent 720ES. A NMR spectrometer was carried out on a Bruker Avance NEO 600.

Electrochemical measurements: The electrochemical tests were carried out using the electrochemical workstation (CHI 660E) in three-electrode cell using carbon rod and Hg/HgO electrode as counter electrode and reference electrode, respectively. All potentials in polarization curves were obtained with iR compensation using the equation: $E_{(iR\text{-compensated})} = E - iR$, where i is the current and R is the uncompensated electrolyte ohmic resistance measured by electrochemical impedance spectroscopy. To obtain the working electrode, catalysts (2 mg) were dispersed into isopropanol (100 μL), deionized water (850 μL) and Nafion (50 μL) by ultrasound for 20 min, and then catalyst ink (5 μL) was dropped onto clean glass carbon electrode (GCE, 0.071 cm^2). The electrochemically active surface area (ECSA) of samples was determined from cyclic voltammetry (CV) by measuring the Pd oxide reduction peak under the deposition potential. The FOR performance of catalysts was evaluated from CV curves tested in 1 M KOH + 0.5 M HCOOK. The HER performance was estimated from linear scanning voltammetry (LSV) measured at 5 mV s^{-1} in 1 M KOH electrolyte. The electrochemical impedance spectroscopy (EIS) was performed in the range of 100 kHz to 100 mHz at -1.6 V. In two-electrode system, catalysts ink was dispersed onto carbon paper (CP) as both anode and cathode, with the mass loading of about 1 mg cm^{-2} . All potentials were transformed to reversible hydrogen electrode (RHE). The current density was normalized to the geometric area of GCE.

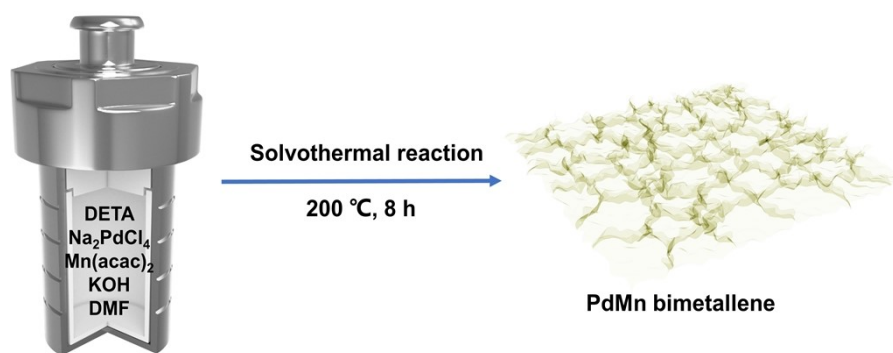


Fig. S1 Schematic illustration of the synthetic process for the PdMn bimetallic.

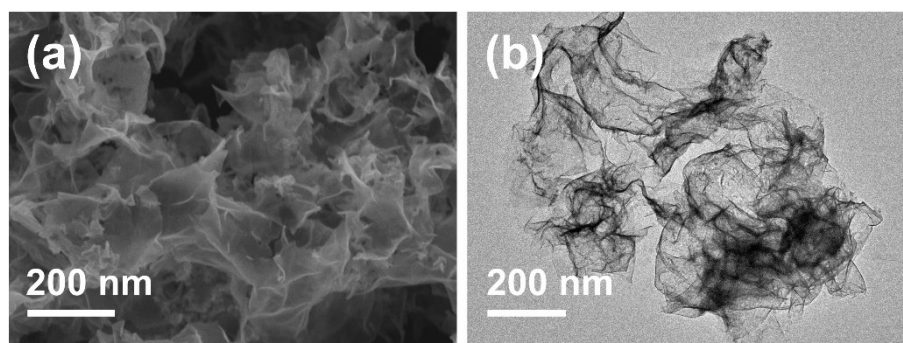


Fig. S2 (a) SEM and (b) TEM images of Pd metallene.

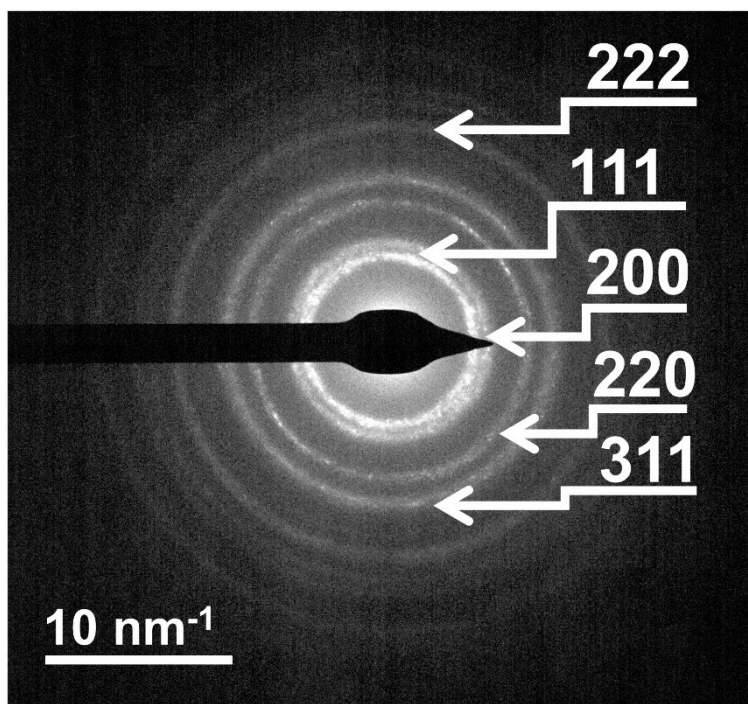


Fig. S3 SAED pattern of PdMn bimetallic.

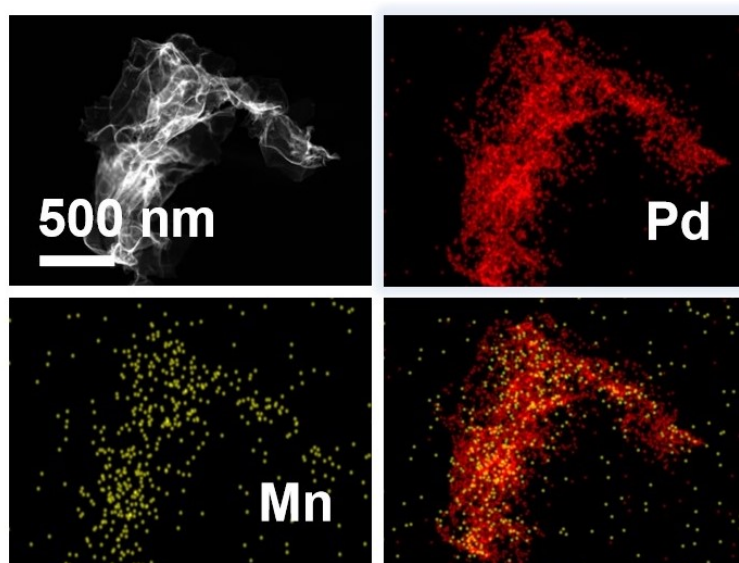


Fig. S4 Elemental mapping of PdMn bimetallic.

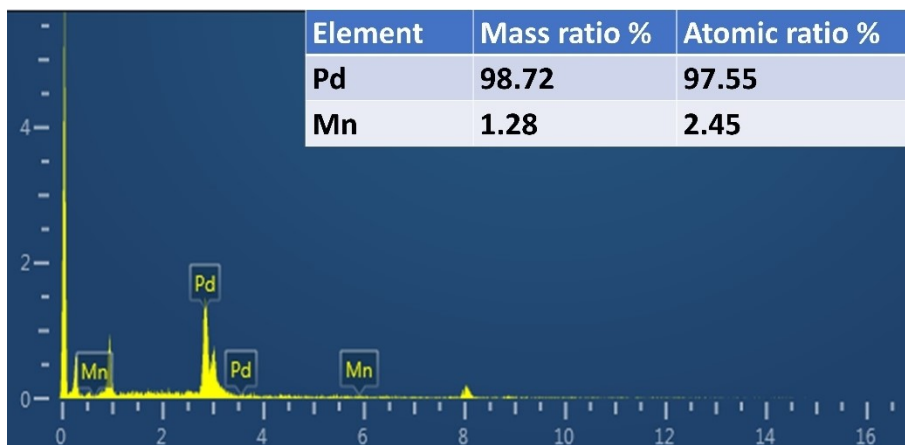


Fig. S5 EDX spectrum of PdMn bimetallic.

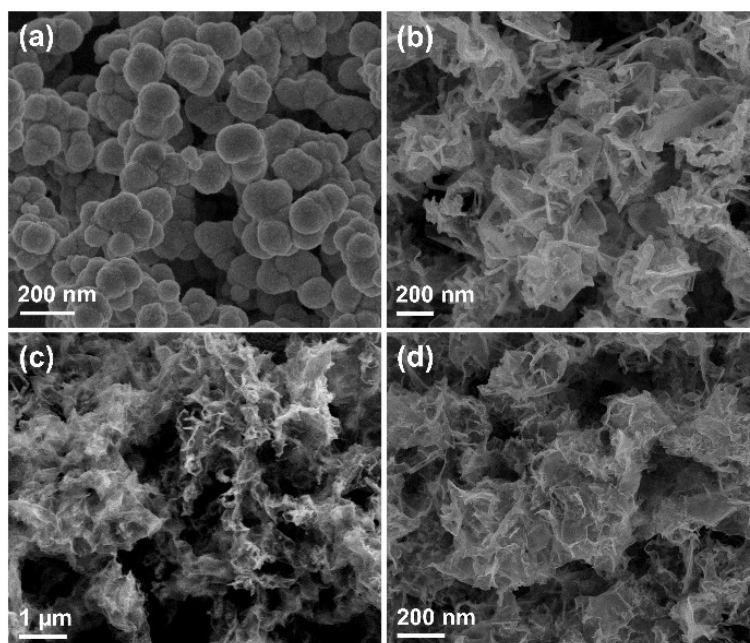


Fig. S6 SEM images of samples prepared with different amounts of KOH: a) 0 g, b) 0.5 g, c) 1 g, and d) 1.5 g.

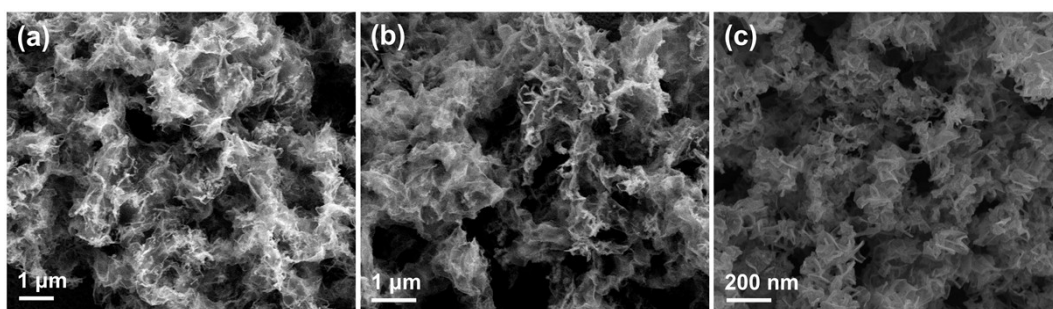


Fig. S7 SEM images of samples prepared with different amounts of Mn(acac)₂: a) 2.5 mg, b) 5 mg and c) 7.5 mg.

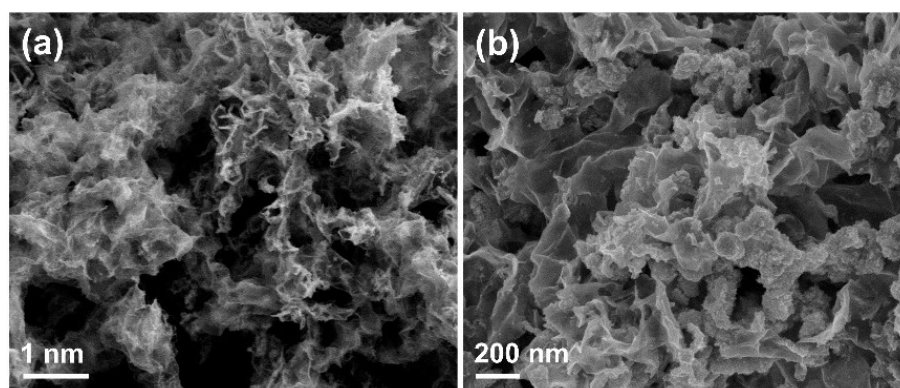


Fig. S8 SEM images of the PdMn bimetallics prepared with different amounts of Mn precursors: a) Mn(acac)₂ and b) MnCl₂.

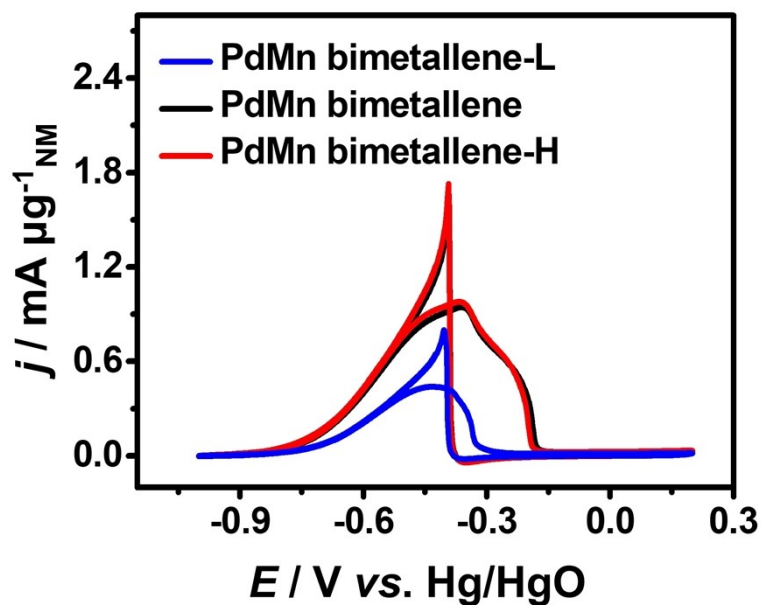


Fig. S9 Mass-normalized CV curves of samples prepared from different amounts of $\text{Mn}(\text{acac})_2$ in N_2 -saturated 1 M KOH + 0.5 M HCOOK at 50 mV s^{-1} .

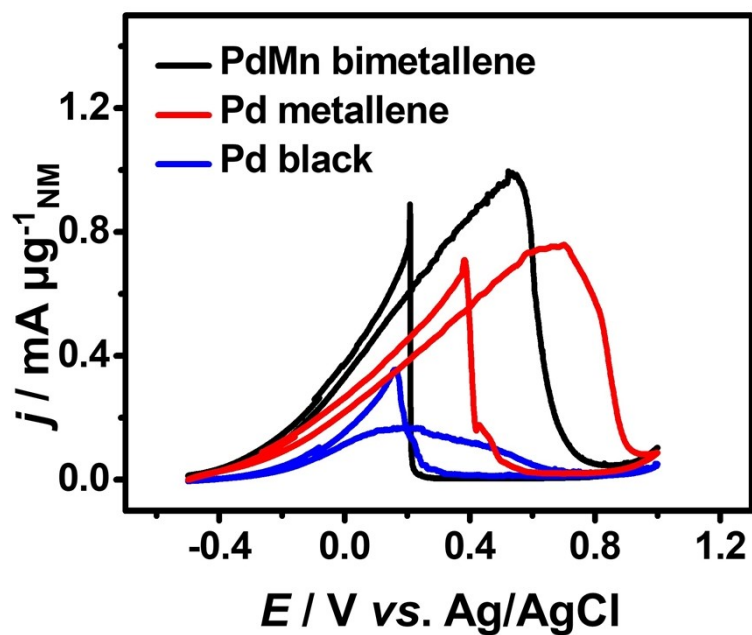


Fig. S10 Mass-normalized CV curves of samples in N_2 -saturated 1 M PBS + 0.5 M HCOOK at 50 mV s^{-1} .

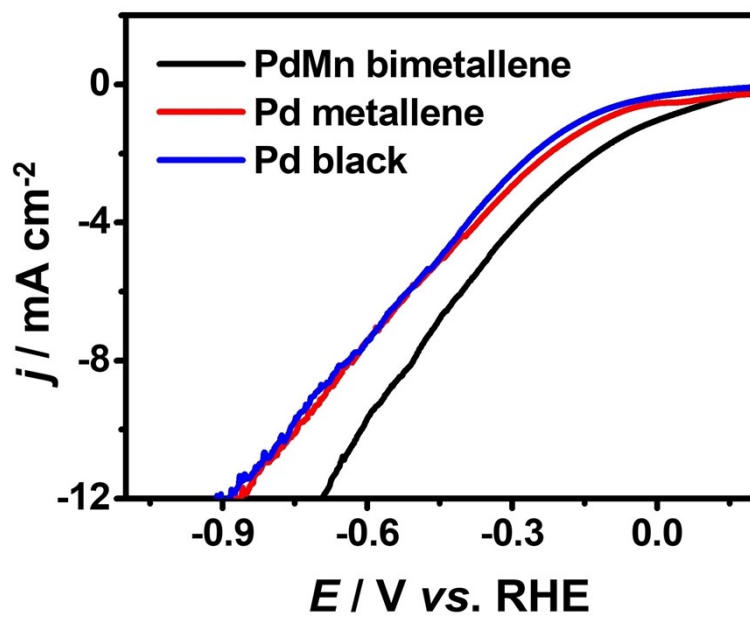


Fig. S11 LSV curves of samples in N_2 -saturated 1 M PBS at 5 mV s^{-1} .

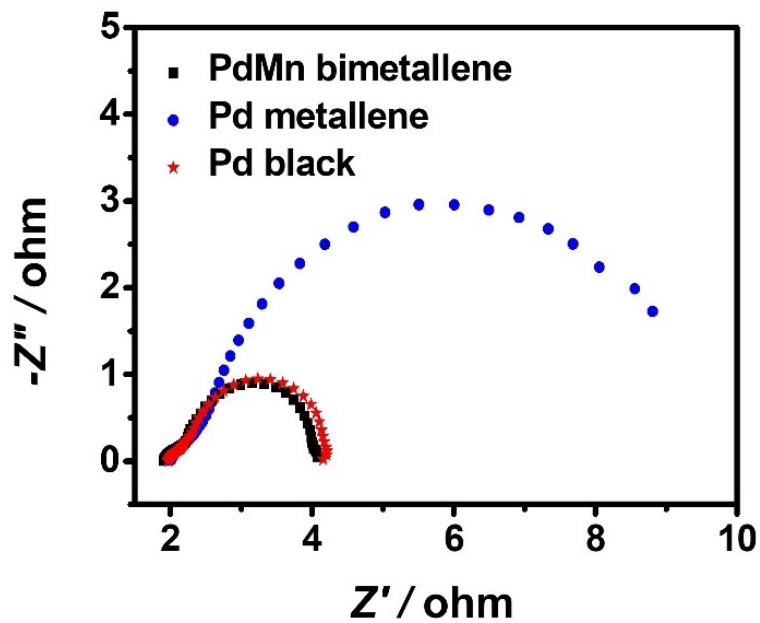


Fig. S12 EIS curves for PdMn bimetallic, Pd metallene, and Pd black in 1.0 M KOH.

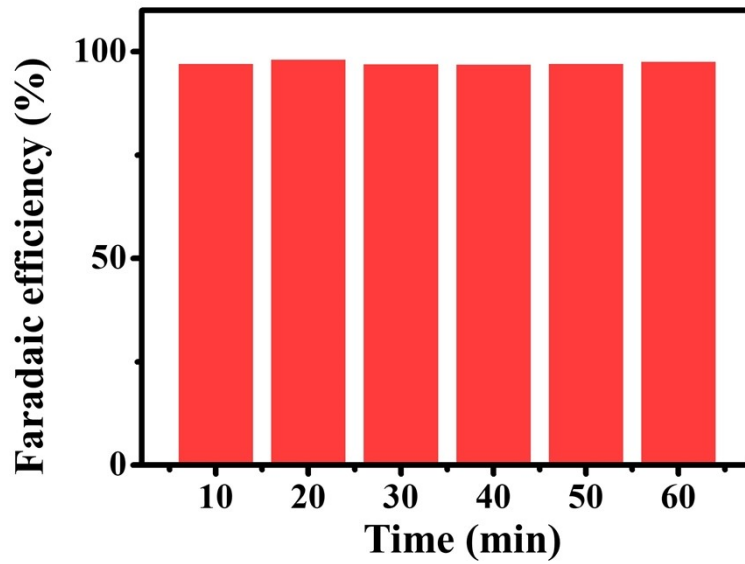


Fig. S13 The Faradaic efficiency of the PdMn bimetallic at current density of 20 mA cm^{-2} .

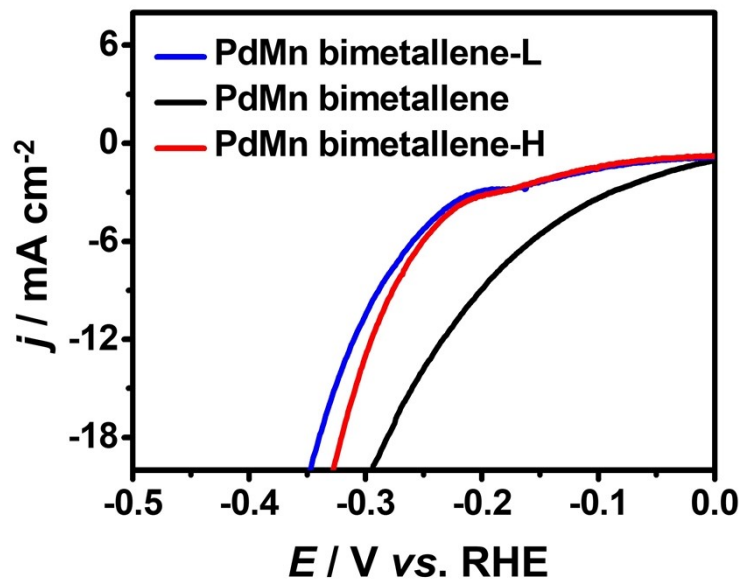


Fig. S14 (a) LSV curves of samples with different amounts of $\text{Mn}(\text{acac})_2$ in N_2 -saturated 1 M KOH at 5 mV s^{-1} .

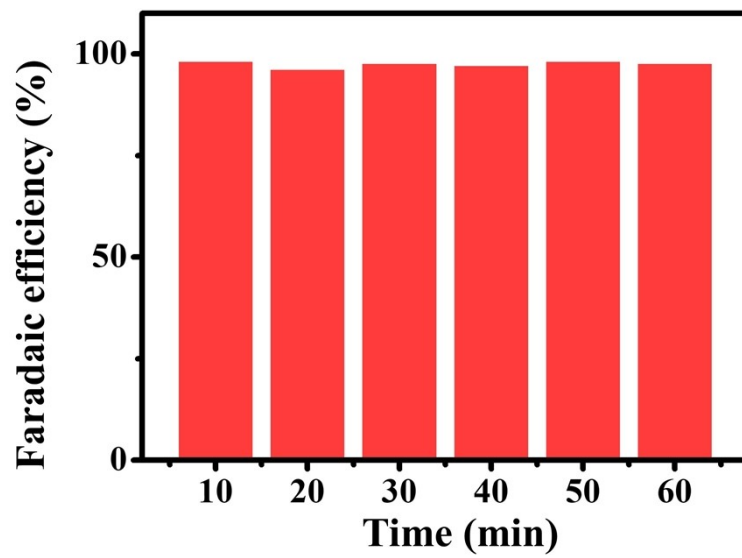


Fig. S15 The Faradaic efficiency of the PdMn bimetallic alloy for HER-FOR at current density of 20 mA cm⁻².

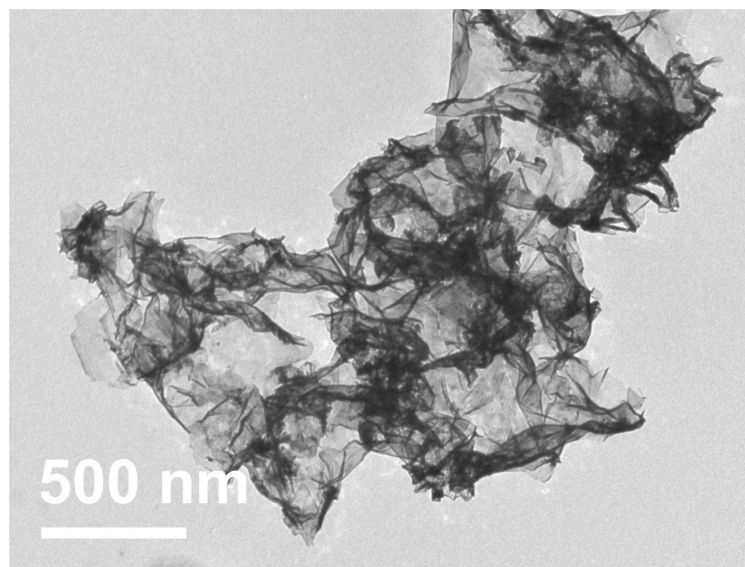


Fig. S16 TEM image of PdMn bimetallic alloy after stability test.

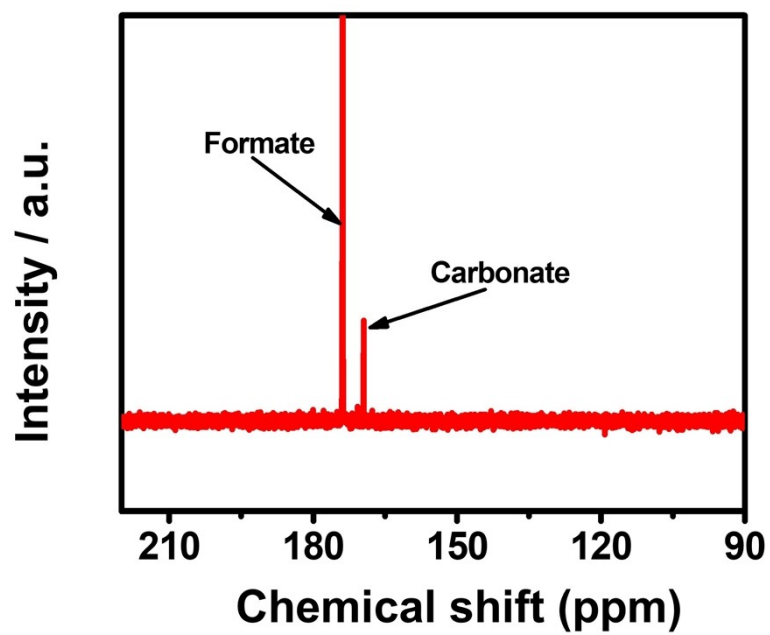


Figure S17. ^{13}C NMR spectra of electrolyte after 10 h anodic oxidation in N_2 -saturated 5.0 M HCOOK + 1.0 M KOH on PdMn bimetallic electrode.